2024 IEEE/RSJ International Conference on Intelligent Robots and Systems (IROS)
October 14-18, 2024. Abu Dhabi, UAE

BEV Image-based Lane Tracking Control System for Autonomous Lane Repainting Robot

Junghyun Seo[1,**], Hyeonjae Jeon[1,**], Joonyoung Choi[1], Kwangho Woo[2], Yongseob Lim[1,†] and Yongsik Jin[3,†]

***Abstract*— In this paper, we present a novel study on a BEV (bird's eye view) image-based lane tracking control system for an autonomous lane repainting robot. Our research introduces a cutting-edge lane detection method based on BEV images, leveraging row-anchor techniques to enhance precision and provide detailed error information for lane tracking algorithms. By utilizing real-time sensor data and advanced deep learning processes, we have successfully implemented a high-performance lane repainting system that minimizes errors and ensures accuracy. Our proposed position-based visual pure pursuit algorithm (PV-PP) plays a crucial role in guiding the lane repainting process with precision and efficiency, ultimately improving the functionality and feasibility of the linear actuator responsible for paint spraying in the real indusrial fields. Through our contributions, including innovative lane detection methods, real-time sensor utilization, and robot control algorithm design, we aim to advance the field of autonomous lane repainting robots and enhance the safety and effectiveness of road maintenance operations.**

I. INTRODUCTION

Roads serve as crucial infrastructure for passengers and freight transportation, promoting various services on transport and reducing trade costs. However, roads are susceptible to damage from various natural disasters or wear and tear over time. Therefore, continuous maintenance is necessary to sustain the benefits of roads, involving activities such as lane painting, crack sealing, road paving, and signage installation, and so on [1]–[3]. Meanwhile, road maintenance process should ensure the safety of all road users, requiring ongoing efforts to meet specific requirements.

As aforementioned, road maintenance is essential for smooth and safe road usage. However, due to the inherently high risks associated with such tasks, careful consideration for the safety of surrounding traffic and workers is necessary. Recent studies indicate an increasing trend in injuries and fatalities on highways and construction sites [4]–[6]. Also, existing method on road marking process in Korea has traditionally been fully manual manner, resulting in frequent casualties. According to statistics from the Korea Road Traffic Authority [7], there have been 170 accidents in highway work zones over the past five years, resulting in 50 fatalities, with a fatality rate three times higher than general traffic accidents (31% versus 9.9%). On the other hand, our unmanned road painting robot autonomously performs lane repainting tasks, reducing job hours compared to manual methods. The proposed robot can ensure worker safety and minimizes traffic congestion time by automating the lane repainting process based on its mobility and autonomy.

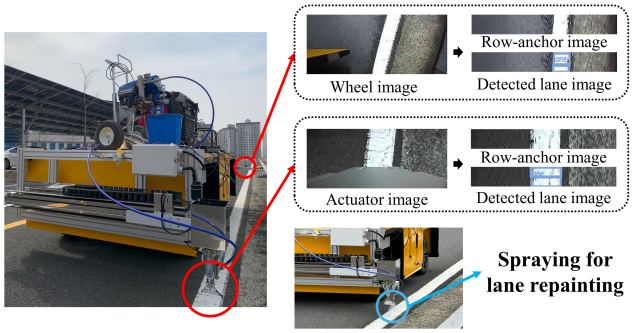

Fig. 1. The images obtained from two camera equipped at the front wheel and the actuator, respectively. Once an image is captured from each camera, our novel lane detection method preprocess the image into row-anchors and perform lane detection on the processed row-anchors. This contributes to precise distance computation for error derivation.

Lane maintenance robots with mobile robots have been developed and used in various manners. There are robots by industrial companies such as STiM [8] and TinyMobileRobot [9], which simultaneously paint lanes while driving on a given route. However, they mainly use GPS-based autonomous driving, and such driving method implies that the limitations of GPS sensors could almost render autonomous driving impractical, potentially hampering overall work efficiency. The GPS signal lost problem usually occurs in areas blocked by building and in tunnel [10]–[12]. These problems are primarily cause of the decreased accuracy in the operation of GPS-based lane maintenance robots. Although GPS-based lane maintenance robots operate well in expansive areas such as open fields and highways, they have limitations that cannot perform in certain urban and tunnel environments [13]. Therefore, lane maintenance operations cannot be performed in locations where precise positioning data like RTK-GPS is not received.

The limitations of GPS can restrict the applicability and capacity of lane repainting robots, and potentially diminish

This work was supported by the Electronics and Telecommunications Research Institute (ETRI) through the Korean Government [24ZD1130, Regional Industry ICT Convergence Technology Advancement and Support Project in Daegu-GyeongBuk (Robot)], and the Commercialization Promotion Agency for R&D Outcomes (COMPA) grant funded by the Korean Government (Ministry of Science and ICT, RS-2023-00304776). It was also supported by the National Research Foundation of Korea (NRF) grant funded by the Korea government (MSIT) (No. 2021R1F1A1046197).

** Equal contribution.
† Corresponding authors.
[1]Junghyun Seo, Hyeonjae Jeon, Joonyoung Choi, and Yongseob Lim are with Daegu Gyeongbuk Institute of Science and Technology (DGIST), Daegu, Republic of Korea. junghyun3607@dgist.ac.kr, wjsguswo12@dgist.ac.kr, cjy9870@dgist.ac.kr, and yslim73@dgist.ac.kr
[2]Kwangho Woo is with Robot for People (RP), Daegu, Republic of Korea. eujin2woo@gmail.com
[3]Yongsik Jin is with Electronics and Telecommunications Research Institute (ETRI), Daegu, Republic of Korea. yongsik@etri.re.kr

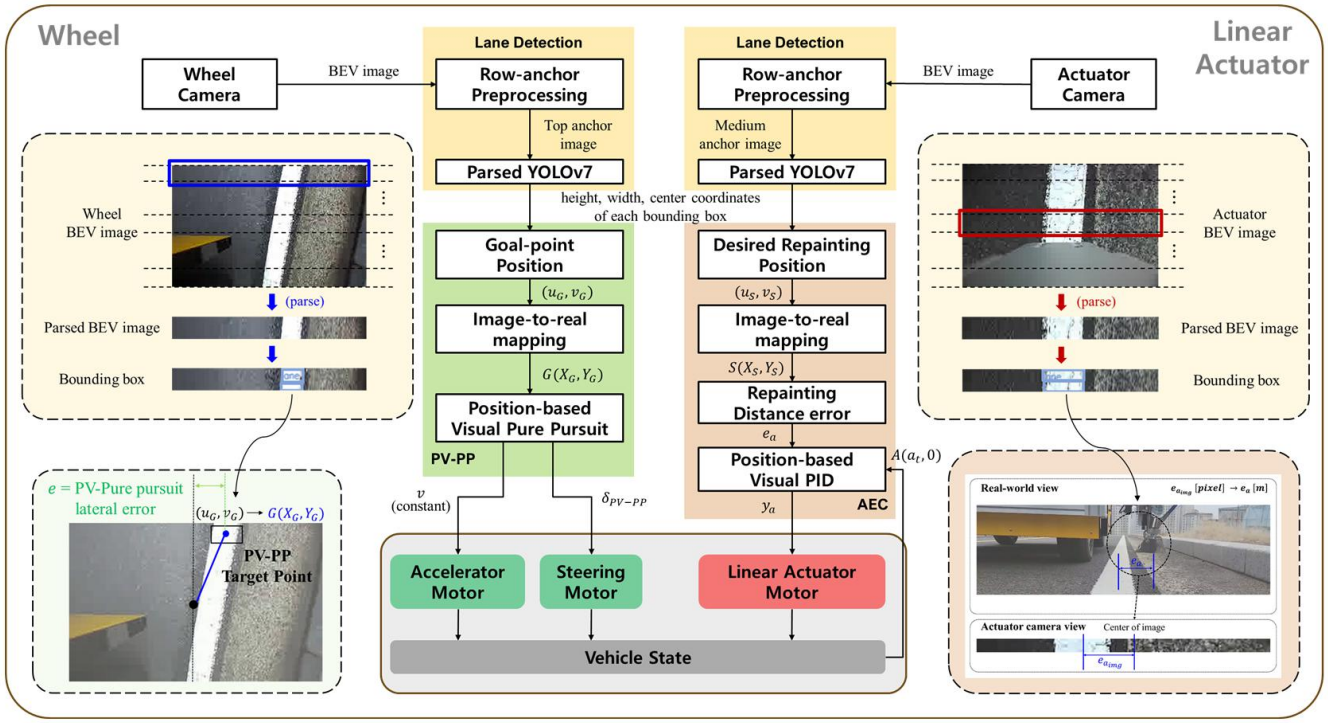

Fig. 2. The system architecture of our lane repainting robot (LP-BOT). The integrated control system is built on ROS and operates at 20Hz, enabling the our robot to perform real-time lane repainting tasks. This system receives image inputs from camera sensors, processes perception and decision tasks, and controls the our robot and repainting device (linear actuator).

operational efficiency of the workflow on the roads. Thus, we have conceived a lane repainting robot that operates based on vision sensors to track existing lanes for lane maintenance, repainting, and lane marking repair tasks. Our proposed robot utilizes image data and their belonging lane information to implement a versatile position-based visual servo control system, which encompasses vehicle navigation control and actuator control for paint spraying during maintenance process. To take advantage of image data and pixel-based rich information, the BEV-like camera sensor configuration is constructed and contributes to the precise detection and tracking of road lanes [14], [15]. Fig. 1 shows an operational scene of our lane repainting robot and the roles of each image according to the camera configuration.

In this paper, we present the lane repainting robot equipped with only camera sensors and independent of the intrinsic limitations followed by the usage of GPS sensors. To facilitate the maintenance and re-striping of existing lanes, our robot demonstrates a simple, yet highly precise detection and tracking control performance based on BEV image data obtained from downward-facing camera settings. The main contributions of this study are as follows:

- To fully take advantage of BEV image, we propose a novel lane detection method based on row-anchor that differentiate specific areas from BEV image. Through this method, the perception model can primarily reduce the lateral error, and transmit more informative and precise errors to the lane tracking algorithm.
- From the image plane of the cameras, we extract the real-world distance information for PV-PP and actuator compensation algorithm. Through these algorithms, we successfully reduce the lane tracking error for high performance lane repainting process (with 4.23mm and 2.70mm of RMSE in each scenario).
- Our novel BEV image-based lane tracking control system is achieved with real-time sensor data and deep learning task processing in the ROS environment [16]. It enables fast and precise lane repainting operations on embedded computing board.
- To enhance the performance of lane repainting, we have developed and adapted actuator error compensation algorithm for the linear actuator that moves the sprayer of the painting robot.

II. Methodology

In this study, we design novel position-based visual pure pursuit algorithm to execute precise lane repainting task. The overall flowchart of our work is depicted in Fig. 2. All cameras are mounted downward to accurately perform lane detection/tracking and image-to-real world mapping has been conducted to convert pixel units from image plane to meter unit in the real environment. The estimated position of lane obtained by row-anchor lane detection is utilized for setting goal point of PV-PP. And then, minimizing errors during lane paint spraying by controlling the linear actuator through an actuator error compensation algorithm. Details of the variables are summarised in Table 1.

A. Novel Lane Detection for BEV Image with Row Anchor

Our robot is designed for lane repainting tasks, utilizing BEV images to achieve higher precision in lane position error

TABLE I

PARAMETER DEFINITIONS AND THEIR CORRESPONDING VALUES.

Parameter	Definition [Unit]	Value
f_x^w	Focal length of the wheel camera along the x-axis[m]	132.44
f_y^w	Focal length of the wheel camera along the y-axis[m]	132.37
f_x^a	Focal length of the actuator camera along the x-axis[m]	132.40
f_y^a	Focal length of the actuator camera along the y-axis[m]	132.31
(c_x^w, c_y^w)	Principal point for 336×188 wheel camera image [pixel]	(164.9, 95.5)
(c_x^a, c_y^a)	Principal point for 336×188 actuator camera image [pixel]	(166.6, 96.2)
z_w	Depth value of front wheel camera [m]	0.592
z_a	Depth value of actuator camera [m]	0.306
Wb	Wheelbase [m]	1.9
h'	Vertical distance from wheel camera to front wheel [m]	0.7
h	Vertical distance from rear wheel to actuator camera [m]	0.5
$G(X_G, Y_G)$	The goal point in real-world coordinates [m]	(varies)
$S(X_S, Y_S)$	Desired spraying point in real-world coordinates [m]	(varies)
$A(a_t, 0)$	X-coordinate and Y-coordinate of the current actuator position [m]	(varies)
δ_{PV-PP}	PV-PP steering angle [deg]	(varies)
a_t	Position of the spraying actuator in translated coordinate [m]	p_w - p_t
e_a	Lateral error of the spraying actuator [m]	X_S
y_a	PID output of the actuator control input value [m]	(varies)
$\bar{y}_a$	Actuator error compensation input [m]	(varies)

calculation for driving and lane repainting operations. For lane detection, the robot obtains BEV images from wheel cameras, as illustrated in Fig. 3. For real-time application, we attempted to employ state-of-the-art (SOTA) deep learning-based lane detection methods such as UFLD [17], LaneATT [18], and CLRNet [19]. However, the majority of existing lane detection algorithms often define anchors or conduct segmentation using images obtained from forward cameras [20]–[22]. In BEV images shown in Fig. 3(a), front-view image-based methods lead to mispredictions caused by the assumption that lanes locate on the anchors optimized to lane positions in front-view images. Therefore, we present novel lane detection method with a preprocessing technique satisfying high precision, given by the BEV image.

YOLOv7 [23] model is employed for lane detection, enabling fast lane recognition on ROS-based embedded computing boards. But if we use the object detection network for lane detection task, the resolution of lane recognition decreases as illustrated in Fig. 3(b). Therefore, as shown in Fig. 3(c), we divide each image into multiple row anchors to increase the resolution of error prediction and implement a lane detection network trained on our custom dataset to predict lane locations from the parsed image. The network outputs two shallow bounding boxes in each anchor so that it can deliver a pixel coordinate of the center of the current location of lane by calculating the average values of the x and y pixel coordinates.

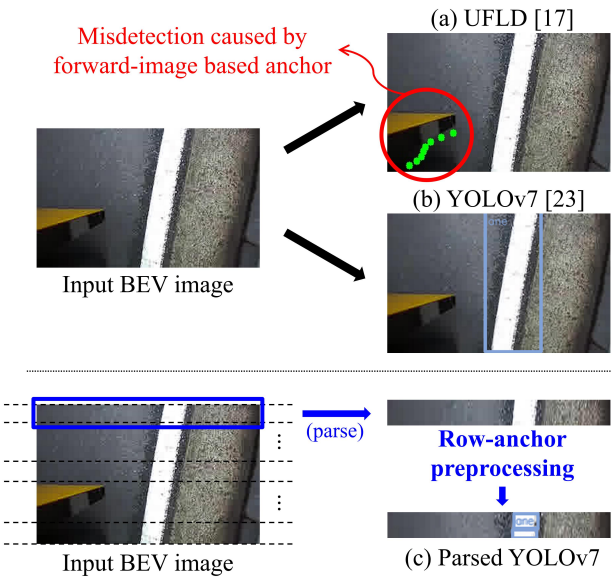

Fig. 3. The input BEV image obtained from the wheel camera and different results from each lane detection method. (a) Conventional SOTA lane detection fails to detection a lane on the BEV image. (b) YOLOv7 based lane detection approach detects the lane with poor error resolution. (c) To improve the resolution of the control error terms, the input image is preprocessed into multiple row anchors with smaller heights.

In the lane detection process, two types of row anchors are utilized and the pixel coordinates of the lanes obtained from these anchors are transferred to image-to-real world distance mapping module: the top anchor from the wheel camera, which serves as the target point during vehicle operation; and the mid anchor from the actuator camera, which is utilized to compute errors for actuator compensation in PV-PP and actuator error compensation algorithm. Algorithm 1 explains how our system integrates YOLOv7 with ROS, publishing pixel coordinates of target point obtained from each image.

Algorithm 1 Lane detection processing with YOLOv7 model in ROS

Input: BEV camera image img
Initialize: lane bounding box B_{img}, processed anchor image img', coordinates of bounding box u, v
Set: ROS publisher p, start row position r, height of row anchor h
Require: pre-trained YOLOv7 lane detector L
while ROS is not shutdown **do**
  $img' \leftarrow img$[r:r+h, :, :]
  $B_{img} \leftarrow L(img')$
  if B_{img} is not empty **then**
    $u, v \leftarrow B_{img}$
  else
    $u, v \leftarrow$ last_u, last_v
  end if
  ros_publish_msg $\leftarrow (u, v)$
  p.publish(ros_publish_msg)
  last_u, last_v $\leftarrow u, v$
end while

B. Image-to-Real World Distance Mapping

To apply control algorithms using the lane position obtained from each anchor, it is necessary to convert the pixel-based coordinates of lane positions obtained in the image coordinate system to real-world coordinates in meters [24]–[26]. We perform image-to-real world distance mapping based on camera matrix to utilize the lane information in the real world domain by the following equation:

$$Z\begin{bmatrix} U \\ V \\ 1 \end{bmatrix} = \begin{bmatrix} f_x & 0 & c_x \\ 0 & f_y & c_y \\ 0 & 0 & 1 \end{bmatrix} \begin{bmatrix} X \\ Y \\ Z \end{bmatrix} \tag{1}$$

where (U, V) represents the image coordinate, and (X, Y, Z) denotes the real-world coordinate as shown in Fig. 4. Expanding (1) with regard to the target point of the vehicle and the desired spraying point, we can perform image-to-real world distance mapping as follows:

$$G_{img}(X_{G_{\text{img}}}, Y_{G_{\text{img}}}) = \left(\frac{z_w(u_G - c_x^w)}{f_x^w}, \frac{z_w(v_G - c_y^w)}{f_y^w} \right) \tag{2}$$

$$S_{img}(X_{S_{\text{img}}}, Y_{S_{\text{img}}}) = \left(\frac{z_a(u_S - c_x^a)}{f_x^a}, \frac{z_a(v_S - c_y^a)}{f_y^a} \right) \tag{3}$$

where $G_{img}(X_{G_{\text{img}}}, Y_{G_{\text{img}}})$ represents the goal point in image-plane coordinates with meter unit, and $S_{img}(X_{S_{\text{img}}}, Y_{S_{\text{img}}})$ denotes the desired spraying point in image-plane coordinates with meter unit.

C. Position-based Visual Pure Pursuit Algorithm (PV-PP)

In this paper, the lane tracking task of the lane repainting robot is performed based on the position of detected lane for BEV image with row anchor and image-to-real world distance mapping. As depicted in Fig. 5., the lane location (u_G, v_G) detected from the wheel image is transformed to $G_{img}(X_{G_{img}}, Y_{G_{img}})$, and the lane location (u_S, v_S) detected from the actuator image is transformed to $S_{img}(X_{S_{img}}, Y_{S_{img}})$. And then, goal point $G(X_G, Y_G)$ is defined by the following equation:

$$G(X_G, Y_G) = (X_{G_{\text{img}}},\ h + Wb + h' + Y_{G_{\text{img}}}) \tag{4}$$

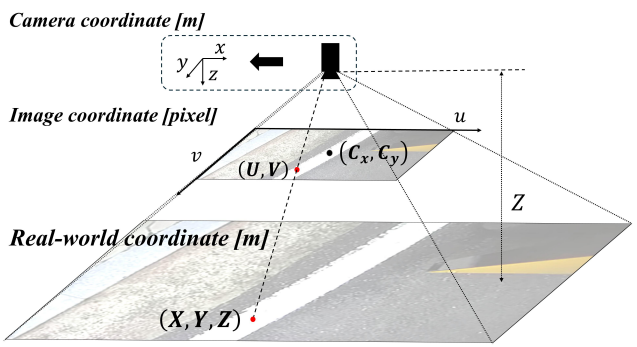

Fig. 4. Image-to-real world mapping example with the lanes on the image coordinate and on the real-world coordinate.

We propose a PV-PP to move the lane repainting point to the goal point in a continuous curve. As shown in Fig. 5(a), the wheel camera is mounted at the front wheel of the repainting robot, and the actuator camera is mounted at the rear part of the repainting robot with its position being the same as the lane repainting point. Since the objective of this study is to minimize errors during lane repainting, the lane repainting point $A(a_t, 0)$ should be positioned at the goal point $G(X_G, Y_G)$ during vehicle autonomous driving.

As shown in in Fig. 5(b), we assume a virtual lane by translating the lane repainting point and the goal point into translated coordinates centered on the middle of repainting robot with a parallel translation of T. The lane repainting point $A(a_t, 0)$ translates to $A'(a_{t'}, 0)$, and the goal point $G(X_G, Y_G)$ translates to $G'(X_{G'}, Y_{G'})$. In this case, it makes sense that when A' reaches G', A also reaches G. The traditional pure pursuit algorithm [27] is designed for the center of rear wheels to reach G', which differs slightly from the objective of this study. It cannot reflect of the current position of the actuator, thereby causing unnecessary errors at the actuator. Thus, considering the relative position of the current actuator position to the desired lane repainting point captured by the actuator camera, we propose PV-PP to move the lane repainting point A to the goal point G.

Through PV-PP algorithm shown in Fig. 6, the steering angle of the vehicle is computed as follows:

$$sin\alpha = \frac{e}{L_d} \tag{5}$$

$$\frac{2sin\alpha cos\alpha}{L_d} = \frac{cos\alpha}{R} \tag{6}$$

$$h'' = h + Wb, \quad h''' = h + Wb + h' + Y_G \tag{7}$$

$$e = \frac{|h''X_G + a_t h''' - a_t h''|}{L} \tag{8}$$

$$\frac{1}{R} = \frac{2sin\alpha}{L_d} = \frac{2e}{{L_d}^2} \tag{9}$$

$$\delta = arctan(\frac{L}{R}) = arctan(\frac{2L}{{L_d}^2}e) \tag{10}$$

In the traditional pure pursuit, assuming the repainting robot as a bicycle model, the grey rectangle representing the center of rear wheel moves to goal point in Fig. 6. To address error of lane tracking, we translate the center of rear wheel into the lane repainting point, and then used modified kinematic model for pure pursuit considering time-varying position of the actuator. The lane repainting point moves towards the goal point following the curvature R of the arc, and the steering angle δ is calculated as in eq (10). The blue rectangle represents the image plane obtained from the wheel camera, and $X_{G_{img}}, Y_{G_{img}}$ are the coordinates of the image converted to real-world coordinates using eq (1). By applying the proposed PP-PV algorithm, the lane repainting point $(a_t, 0)$ moves to $(X_{G_{img}},\ h + Wb + h' + Y_{G_{img}})$, reducing lane repainting errors through vehicle operation.

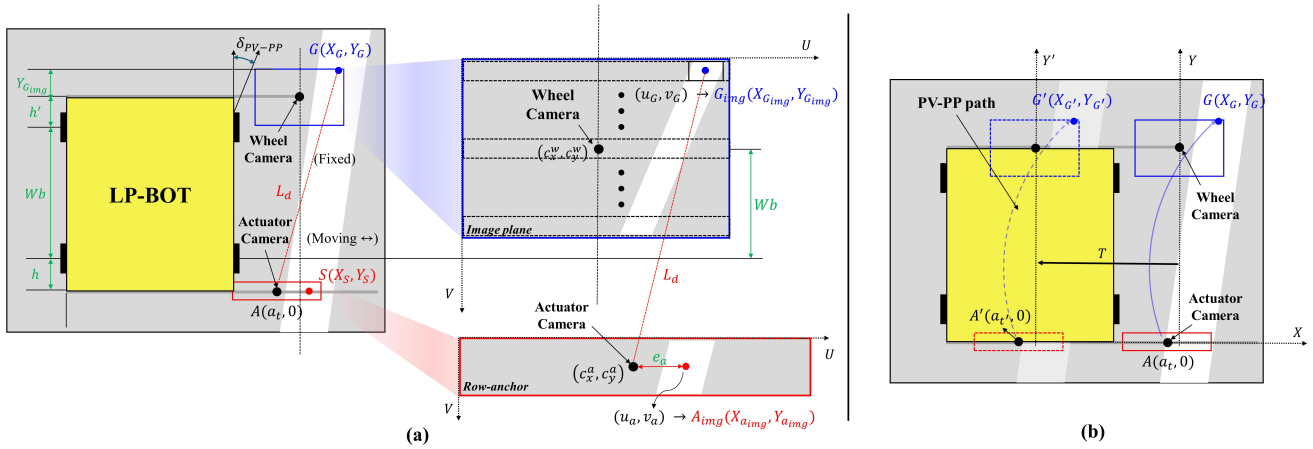

Fig. 5. The architecture of our lane repainting robot (LP-BOT). (a) provides an camera image information of LP-BOT. The wheel camera and actuator camera are mounted at differnet positions on the vehicle. Lane detection for BEV images from both cameras with row anchor is performed to estimate the lane positions. Subsequently, image-to-real world distance mapping is conducted to estimate error distance in the real-world coordinates. (b) shows the path calculated by PV-PP algorithm.

D. Actuator Error Compensation Algorithm

Although we can reduce the actuator error by considering the relative position of the actuator and the wheel BEV camera, there is an intrinsic bias due to the disturbances that occurs during the vehicle operation. To compensate the error caused by large variation and delay of the sensor data, we propose the actuator error compensation algorithm. As depicted in Fig. 5(a), the repainting error e_a is defined as a distance from the current position of the spraying point to the detected lane in actuator camera. e_a can be represented by following equation:

$$e_a = ||A - S||_2 = \sqrt{(X_S - a_t)^2 + Y_S^2} \tag{11}$$

$$y_a(t) = K_p e_a(t) + K_i \int e_a(\tau)\, d\tau + K_d \frac{de_a(t)}{dt} \tag{12}$$

The actuator camera is mounted on the same position as repainting point, and repainting point is controlled by PID-based position controller in the linear actuator. Thus, proposed PV-PP based driving performance contributes to an initial decrease in e_a, while the linear actuator's operation enabling simultaneous compensation of e_a to minimize the repainting error distance. PID-based position controller is constructed in eq (12), which reduce the actuator error successfully.

III. Experiment

In this study, we construct the lane repainting robot (LP-BOT) to perform the autonomous driving lane repainting task and conduct experiments accordingly. The systemic architecture of the LP-BOT system is depicted in Fig. 2, and two cameras are mounted at the right wheel and on the linear actuator. Respectively, the robot obtains the target point of PV-PP algorithm from the wheel image and the lane repainting point from the image at the actuator. The overall integrated control system is built on ROS (Robot operating system) and enables to real-time repainting tasks using deep learning-based lane detection.

A. Implementation Details

Our LP-BOT is a front-wheel drive vehicle that receives speed and steering values via ROS for lane repainting task.

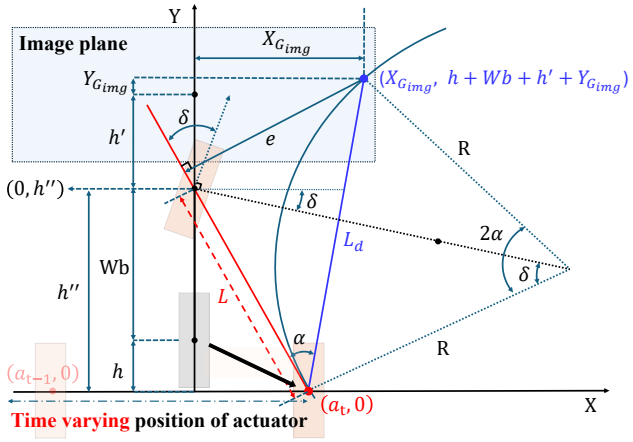

Fig. 6. Position-based visual pure pursuit algorithm.

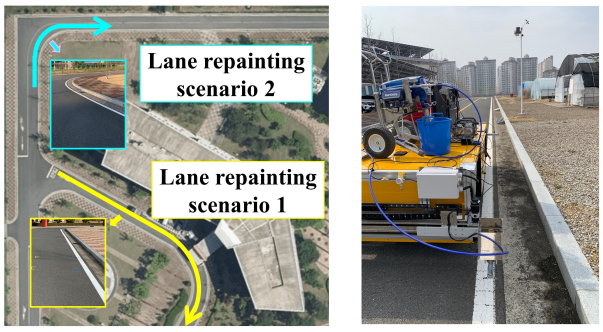

Fig. 7. Examples of lane repainting experiment. (a) represents the lane repainting scenarios, where the lane repainting robot sprays paint along the line within the yellow and sky rectangle. (b) depicts our repainting robot in lane repainting operation.

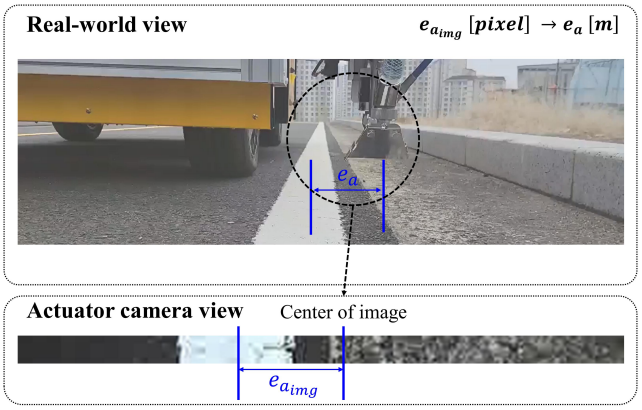

Fig. 8. Examples of lane repainting error in real-world and actuator camera view. Lane repainting error e_a is obtained by transforming image plane error distance $e_{a_{img}}$ into real-world error distance.

All cameras are ZED2i, sending images with a resolution of 336x188 and an FPS of 30Hz. The embedded board utilized for camera package operation and processing is Jetson Orin AGX, with Ubuntu 20.04 OS and ROS Noetic adopted for computing environment setup. The ROS-based integrated control system is depicted in Fig.2, with the frequency of all configured ROS nodes set to 20Hz.

B. Experimental Settings

In this work, experiments are proceeded within Electronics and Telecommunications Research Institute Daegu-Gyeongbuk Research Center. As shown in Fig. 7(a), LP-BOT conducts experiments performing lane repainting tasks on scenario 1 and 2. Scenario 1 consists of long straight and short curve lane sections and scenario 2 is composed of short straight and long curve lane sections. Fig. 7(b) represents LP-BOT equipped with a paint spraying devices, conducting lane repainting tasks in real-world environments. The lane tracking performance have been evaluated by measuring the repainting distance error e_a, demonstrating the effectiveness of the proposed algorithms in this study.

C. Custom Dataset for Parsed YOLOv7 Lane Detection

We construct two custom BEV lane datasets for training the parsed YOLOv7 lane detection model: one for wheel BEV image lane detection and the other for actuator BEV image lane detection. Each dataset includes 3200 training samples, 400 testing samples, and 400 validation samples. Additionally, each sample comprises a parsed real-world BEV image at a resolution of 336x15 along with corresponding lane bounding box label data.

D. Lane Repainting Task Results

As depicted in Fig. 8, the repainting distance error e_a represents the distance from the current position of the spraying point to the detected lane in actuator camera. In this experiment, we used e_a as a metric for the evaluation of lane tracking performance. For two scenarios above, we implement autonomous lane tracking system while minimizing the lane repainting error, and finally evaluate the performance of the overall driving behavior and lane repainting performance based on e_a.

Fig. 9 and Fig. 10 shows the lane tracking performance and the driving behavior of our LP-BOT with different kinds of driving algorithms including original pure pursuit (PP), position-based visual pure pursuit (PV-PP), and PV-PP combined with actuator error compensation (AEC). In the straight section in Scenario 1, the repainting distance error of PV-PP and PV-PP with AEC converges to zero, which means that the robot can appropriately traces the lane that should be maintained or repainted. The result verifies that our proposed PV-PP based driving strategy works better than the original pure pursuit algorithm which moves the rear axle of the vehicle. By adjusting the gap of geometry that comes from the movement of the actuator, we effectively reduced the repainting error. However, when the robot goes through the curved road section, its actuator hardly follows the lane because of a larger curvature. To reflect this additional error, AEC generates a control input for the linear actuator that directly reduces the value of e_a. When performing the lane repainting tasks in scenario 1 using the PP, PV-PP and PV-PP with AEC algorithms, the RMSE, mean, std., max. values of e_a are shown in Table. 2. It is observed that the lane repainting distance error e_a using the presented PV-PP algorithm decreases more than when using the traditional pure pursuit algorithm. Especially, when PV-PP and AEC are used together, it shows a very lower error value, with an RMSE error of 4.23mm, representing a significant decrease of 92.42% compared to the traditional pure pursuit algorithm.

TABLE II

THE LANE TRACKING PERFORMANCE EVALUATED BY MEASURING THE REPAINTING ERROR e_a IN SCENARIO 1.

Method	RMSE [mm]	Mean [mm]	Std. [mm]	Max. [mm]
PP	55.80	42.50	52.76	158.60
PV-PP	48.94	25.96	48.61	141.26
PV-PP + AEC	**4.23**	**2.46**	**4.23**	**19.36**

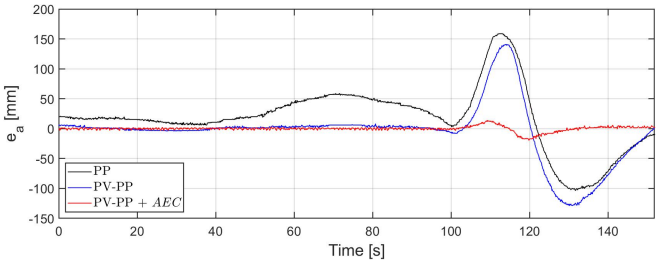

Fig. 9. Lane repainting error e_a of different approaches for Scenario 1.

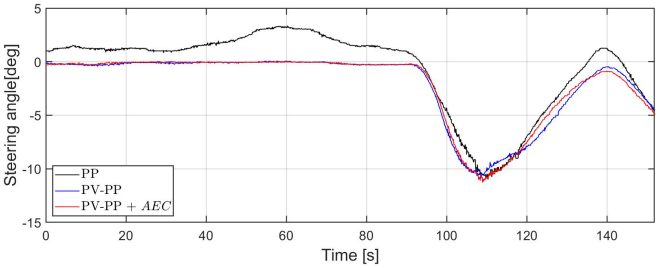

Fig. 10. Steering angle by different driving algorithms for Scenario 1.

TABLE III

THE LANE TRACKING PERFORMANCE EVALUATED BY MEASURING THE REPAINTING ERROR e_a IN SCENARIO 2.

Method	RMSE [mm]	Mean [mm]	Std. [mm]	Max. [mm]
PP	40.20	30.66	27.68	94.47
PV-PP	31.31	22.51	27.06	86.38
PV-PP + AEC	**2.70**	**2.00**	**2.70**	**13.58**

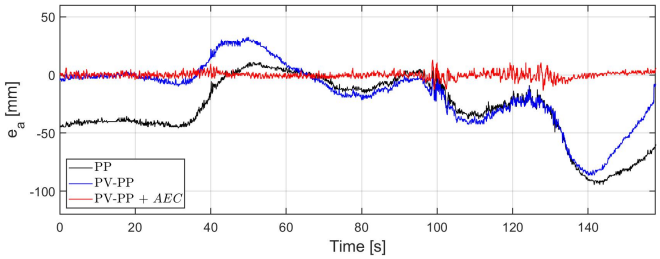

Fig. 11. Lane repainting error e_a of different approaches for Scenario 2.

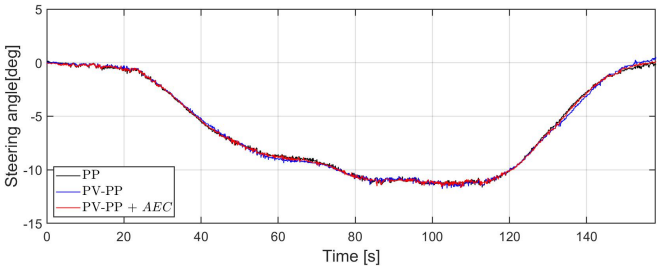

Fig. 12. Steering angle by different driving algorithms for Scenario 2.

Fig. 11 and Fig. 12 shows the lane repainting error and the steering of our robot with different kinds of driving methods. Different from the previous scenario, Scenario 2 is consisted with relatively longer curve lane section. In this case, the orginal PP driving suffers the intrinsic error in both straight and curve road sections. Also, the repainting distance error of PV-PP and PV-PP with AEC goes to zero in the straight roads, but that of PV-PP becomes larger when the robot enters the curved roads. To compensate the error generated by the curvature, AEC attempts to move the actuator to the desired spraying point and it effectively diminishes e_a as shown in Fig. 11. When performing the lane repainting tasks in scenario 2 using the PP, PV-PP and PV-PP combined with AEC algorithms, the RMSE, mean, std., max. values of e_a are shown in Table. 3. it is also shown that the lane repainting distance error e_a using the presented PV-PP algorithm decreases more than when using the traditional pure pursuit algorithm. In this case, when using PV-PP and AEC are used together, RMSE error value is 2.70mm which lower than scenario 2 case, representing a notable reduction of 93.28% compared to the traditional pure pursuit algorithm. The overall lane repainting error level using our algorithm in two scenarios consists of low range with mm units, and our algorithm has over 90% less error than the traditional algorithm, demonstrating that our proposed PV-PP integrated with AEC algorithm can perform very precise lane repainting tasks. Fig. 13 depicts the qualitative result of our proposed method, showing that the lane tracking error of the linear actuator can be significantly reduced by applying AEC.

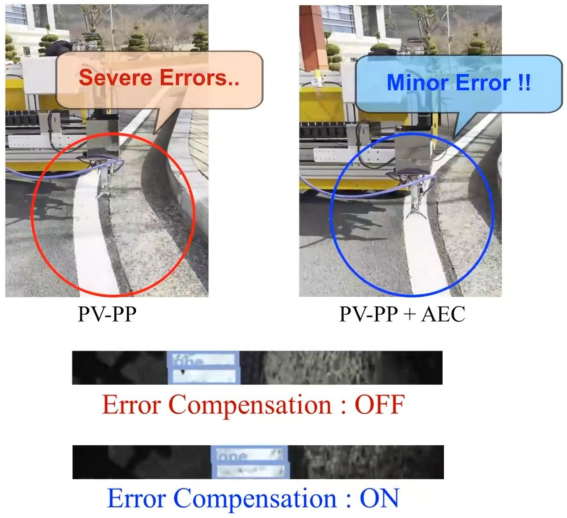

Fig. 13. Qualitative result of the PV-PP combined with AEC. The lane tracking error of the linear actuator significantly decreases when applying AEC.

IV. DISCUSSION AND CONCLUSIONS

In this paper, we describe the necessity for the development of a lane repainting robot based on autonomous driving technology, and conduct experiments to verify its potential usage through systematic implementation. Given the nature of lane repainting tasks, which require very small error of less than 0.01m, we propose lane recognition and robot control utilizing the advantages of Bird's Eye View (BEV) images instead of forward images commonly used in conventional autonomous driving methods. In the process of lane recognition using BEV images, we divide the images into multiple row anchors to enhance the detection resolution of errors used for driving information. We utilize the target point of vehicle movement detected based on parsed lane recognition, and develop a driving algorithm that keeps the desired distance between the autonomous driving robot and the target lane using the pure pursuit algorithm. Specifically, our proposed PV-PP algorithm demonstrates highly accurate lane repainting performance within 3mm, by considering not only the movement of the vehicle but also the real-time position variation of the spraying actuator. Our system is designed based on the ROS middleware and conducts real-time deep learning-based lane recognition, enabling fast and precise lane repainting operations using detected driving and repainting errors. With autonomous lane repainting robots, it is expected to contribute to conducting unmanned lane repainting operations safely, thus enhancing safety at repainting sites where fatal accidents occur without causing disruption to surrounding traffic.

Though our robot successfully detects lanes and traces the lane with small errors based on the BEV images obtained from the downward camera, the limitation of this work is that the performance of the system can be degraded when there is a dashed lane line instead of a continuous lane. For future research, our goal is to design a perception system which is

robust under a temporal absence of lane in the image, and a control system which can adapt to delayed observations caused by dashed lane or unexpected situations.

REFERENCES

[1] A. de Bortoli, A. Féraille, and F. Leurent, "Towards road sustainability—part i: principles and holistic assessment method for pavement maintenance policies," *Sustainability*, vol. 14, no. 3, p. 1513, 2022.

[2] S. Burningham and N. Stankevich, "Why road maintenance is important and how to get it done," 2005.

[3] T. Usman, L. Fu, and L. F. Miranda-Moreno, "Quantifying safety benefit of winter road maintenance: Accident frequency modeling," *Accident Analysis & Prevention*, vol. 42, no. 6, pp. 1878–1887, 2010.

[4] G. M. Waehrer, X. S. Dong, T. Miller, E. Haile, and Y. Men, "Costs of occupational injuries in construction in the united states," *Accident Analysis & Prevention*, vol. 39, no. 6, pp. 1258–1266, 2007.

[5] D. Arditi, D.-E. Lee, and G. Polat, "Fatal accidents in nighttime vs. daytime highway construction work zones," *Journal of Safety Research*, vol. 38, no. 4, pp. 399–405, 2007.

[6] N. J. Goodall, "Comparison of automated vehicle struck-from-behind crash rates with national rates using naturalistic data," *Accident Analysis & Prevention*, vol. 154, p. 106056, 2021.

[7] "Traffic accident statistic analysis," Retrieved from https://taas.koroad.or.kr/web/bdm/srs/selectStaticalReportsDetail.do, 2023.

[8] STiM Company, "Road marking machine stim kontur 700 tpk," 2016.

[9] TinyMobileRobots, "Tinysurveyor tinypremarker introduction," 2019.

[10] K. Mohta, K. Sun, S. Liu, M. Watterson, B. Pfrommer, J. Svacha, Y. Mulgaonkar, C. J. Taylor, and V. Kumar, "Experiments in fast, autonomous, gps-denied quadrotor flight," in *2018 IEEE International Conference on Robotics and Automation (ICRA)*. IEEE, 2018, pp. 7832–7839.

[11] B. H. Kaygisiz, A. M. Erkmen, and I. Erkmen, "Gps/ins enhancement using neural networks for autonomous ground vehicle applications," in *Proceedings 2003 IEEE/RSJ International Conference on Intelligent Robots and Systems (IROS 2003)(Cat. No. 03CH37453)*, vol. 4. IEEE, 2003, pp. 3763–3768.

[12] Y. Cui and S. S. Ge, "Autonomous vehicle positioning with gps in urban canyon environments," *IEEE transactions on robotics and automation*, vol. 19, no. 1, pp. 15–25, 2003.

[13] J. Siva and C. Poellabauer, "Robot and drone localization in gps-denied areas," *Mission-Oriented Sensor Networks and Systems: Art and Science: Volume 2: Advances*, pp. 597–631, 2019.

[14] M. Bai, G. Mattyus, N. Homayounfar, S. Wang, S. K. Lakshmikanth, and R. Urtasun, "Deep multi-sensor lane detection," in *2018 IEEE/RSJ International Conference on Intelligent Robots and Systems (IROS)*. IEEE, 2018, pp. 3102–3109.

[15] R. Wang, J. Qin, K. Li, Y. Li, D. Cao, and J. Xu, "Bev-lanedet: An efficient 3d lane detection based on virtual camera via key-points," in *Proceedings of the IEEE/CVF Conference on Computer Vision and Pattern Recognition*, 2023, pp. 1002–1011.

[16] M. Quigley, K. Conley, B. Gerkey, J. Faust, T. Foote, J. Leibs, R. Wheeler, A. Y. Ng *et al.*, "Ros: an open-source robot operating system," in *ICRA workshop on open source software*, vol. 3, no. 3.2. Kobe, Japan, 2009, p. 5.

[17] Z. Qin, H. Wang, and X. Li, "Ultra fast structure-aware deep lane detection," in *Computer Vision–ECCV 2020: 16th European Conference, Glasgow, UK, August 23–28, 2020, Proceedings, Part XXIV 16*. Springer, 2020, pp. 276–291.

[18] L. Tabelini, R. Berriel, T. M. Paixao, C. Badue, A. F. De Souza, and T. Oliveira-Santos, "Keep your eyes on the lane: Real-time attention-guided lane detection," in *Proceedings of the IEEE/CVF conference on computer vision and pattern recognition*, 2021, pp. 294–302.

[19] T. Zheng, Y. Huang, Y. Liu, W. Tang, Z. Yang, D. Cai, and X. He, "Clrnet: Cross layer refinement network for lane detection," in *Proceedings of the IEEE/CVF conference on computer vision and pattern recognition*, 2022, pp. 898–907.

[20] D. Neven, B. De Brabandere, S. Georgoulis, M. Proesmans, and L. Van Gool, "Towards end-to-end lane detection: an instance segmentation approach," in *2018 IEEE intelligent vehicles symposium (IV)*. IEEE, 2018, pp. 286–291.

[21] N. Garnett, R. Cohen, T. Pe'er, R. Lahav, and D. Levi, "3d-lanenet: end-to-end 3d multiple lane detection," in *Proceedings of the IEEE/CVF International Conference on Computer Vision*, 2019, pp. 2921–2930.

[22] T. Zheng, H. Fang, Y. Zhang, W. Tang, Z. Yang, H. Liu, and D. Cai, "Resa: Recurrent feature-shift aggregator for lane detection," in *Proceedings of the AAAI Conference on Artificial Intelligence*, vol. 35, no. 4, 2021, pp. 3547–3554.

[23] C.-Y. Wang, A. Bochkovskiy, and H.-Y. M. Liao, "Yolov7: Trainable bag-of-freebies sets new state-of-the-art for real-time object detectors," in *Proceedings of the IEEE/CVF conference on computer vision and pattern recognition*, 2023, pp. 7464–7475.

[24] C. Chen, Y. Tian, L. Lin, S. Chen, H. Li, Y. Wang, and K. Su, "Obtaining world coordinate information of uav in gnss denied environments," *Sensors*, vol. 20, no. 8, p. 2241, 2020.

[25] C. Campos, R. Elvira, J. J. G. Rodríguez, J. M. Montiel, and J. D. Tardós, "Orb-slam3: An accurate open-source library for visual, visual–inertial, and multimap slam," *IEEE Transactions on Robotics*, vol. 37, no. 6, pp. 1874–1890, 2021.

[26] B. Kitt, A. Geiger, and H. Lategahn, "Visual odometry based on stereo image sequences with ransac-based outlier rejection scheme," in *2010 ieee intelligent vehicles symposium*. IEEE, 2010, pp. 486–492.

[27] R. C. Coulter *et al.*, *Implementation of the pure pursuit path tracking algorithm*. Carnegie Mellon University, The Robotics Institute, 1992.